Desalination and Water Treatment
www.deswater.com

doi: 10.1080/19443994.2015.1134355

57 (2016) 23940–23950
October

Removal of hexavalent chromium from aqueous solution by a novel biosorbent *Caryota urens* seeds: equilibrium and kinetic studies

E. Suganya, S. Rangabhashiyam, A.V. Lity, N. Selvaraju*

Department of Chemical Engineering, National Institute of Technology Calicut, Kozhikode 673601, Kerala, India, emails: elasuganyame@gmail.com (E. Suganya), rambhashiyam@gmail.com (S. Rangabhashiyam), lityalen@nitc.ac.in (A.V. Lity), Tel. +91 495 2285409; Fax: +91 495 2287250; email: selvaraju@nitc.ac.in (N. Selvaraju)

Received 21 June 2015; Accepted 14 December 2015

ABSTRACT

A novel biosorbent *Caryota urens* seeds (CUS) was investigated for the technical feasibility for the biosorption of hexavalent chromium from aqueous solution. The biosorbent was characterized by SEM, FT-IR spectral, and EDS analysis. Effects of biosorbent size, biosorbent dosage, Cr(VI) concentration, pH, and contact time on the biosorption of hexavalent chromium were investigated. Both the Langmuir and Freundlich isotherms were suitable for describing the biosorption of Cr(VI) onto CUS. Application of the Langmuir isotherm model to the biosorption system yielded a maximum biosorption capacity of 52.63 mg/g at an equilibrium pH value of 2 and 303 K. Kinetic data were best fitted with the pseudo-second-order kinetic model. The results indicate that the CUS can be effective biosorbent for the removal of Cr(VI) from aqueous solution.

Keywords: Biosorption; Hexavalent chromium; *Caryota urens* seed; Isotherms; Kinetics

1. Introduction

More research on water purification is focused because of the shortage in the fresh drinking water, which is the major concern worldwide nowadays [1–4]. The pollutants removal from the various industrial sources is becoming the most vital environmental issue [5–9]. Different techniques on advanced wastewater treatment are concerned to combat the problem [10–15]. Hexavalent chromium is considered as a major pollutant from the effluent streams of various industries such as glass, electroplating, tanning, mining, ceramics, rubber, fertilizers, metallurgical, etc. [16,17]. Cr(VI) is a carcinogenic agent and associated with the various health risks like liver damage, severe diarrhea, nausea, vomiting, and corrosion of skin [18]. The United States Environmental Protection Agency (USEPA) has set the tolerance limit for the Cr(VI) discharge into surface water as 0.1 mg/L and in case of potable water as 0.05 mg/L [19,20]. Removal of hexavalent chromium from wastewater is accomplished by various conventional technologies like chemical precipitation [21], electrochemical reduction [22], membrane separation [23], ion exchange [24], and extraction [25]. The wastewater treatment process is based on the effluent characteristics such as, pH, temperature, metal concentration, the economics, and the social factor like standard set by government agencies [26,27]. Activated carbon is the traditional inorganic adsorbent for wastewater pollutant with its high specific surface area, but its cost factor has restricted its comprehensive applications [28]. So, the development

---

*Corresponding author.

of economical and easily available adsorbents for the heavy metal removal from the aqueous solution is highly necessary. Biosorption is a potential method for wastewater treatment based on the characteristic features of biomasses toward pollutants binding. The merits of biosorption include economical, high efficiency of heavy metal removal from dilute solution and biosorbent regeneration [29,30]. Literature review by the author in nearly all of the peer reviewed journals indicated that biosorption investigation of hexavalent chromium by *Caryota urens* seed (CUS) as a biosorbent has not been employed. Therefore, the present study subjects the novel *C. urens* seed (CUS) toward Cr(VI) removal from aqueous solution.

The present study focuses on the investigation over the effects of pH, contact time, biosorbent dose, biosorbent size, and initial metal ion concentration on Cr(VI) removal using CUS. The equilibrium data obtained in this study are tested with isotherm and kinetic models in order to evaluate the biosorption of Cr(VI) on CUS.

2. Materials and methods

2.1. Preparation of stock solution

An aqueous solution (1,000 mg/L) of Cr(VI) ions was prepared by using $K_2Cr_2O_7$ salt. For pH adjustments, 0.1 N HCL/0.1 N NaOH was used. The stock solution was diluted with distilled water to obtain the desired Cr(VI) concentration range.

2.2. Preparation of biosorbent

The seeds of *C. urens* (CUS) were collected from the local area of Kozhikode. The collected seeds were washed, dried, pulverized, and sieved to obtain the size of CUS in the range of 0.212–0.300 mm. The prepared CUS were kept in air tight plastic bottles. The elemental composition of CUS was found as 41.88% C, 8.17% H, 0.16% S, and 0.33% N. CUS was used as such without any pretreatment.

2.3. Characterization of the biosorbent

The percentage elements composition of the CUS was analyzed using C–H–N Analyzer (Vario EL III, Elementar). The surface functional groups of the CUS were determined through FT-IR spectroscope (Nicolet Avatar 370, Thermo Scientific). The surface morophology of the CUS was studied by SEM (SU6600, Hitachi). The elemental composition of the CUS was determined through EDX analyzer (EMAX-7000, Horiba).

2.4. Batch experiment

The batch biosorption experiments were carried out using 50 ml of Cr(VI) solution with optimum value of pH, biosorbent dosage, biosorbent size, metal ion concentration at 303 K, and agitation speed of 120 rpm on orbital shaker (116736 GB; GeNei). After the desired contact time, the samples were filtered through Whatman No. 1 filter paper and the filtrates were analyzed for residual Cr(VI) ion concentration using double array UV–vis Spectrophotometer (2201; Systronics) by diphenyl-carbazide method [31]. The amount of Cr(VI) ions biosorbed q (mg/g) was calculated by using the following mass balance equation

$$q_e = \frac{C_0 - C_e}{m} \times V \tag{1}$$

and the Cr(VI) percent removal (%) was calculated using the following equation:

$$\text{Removal (\%)} = \left(\frac{C_0 - C_e}{C_0}\right) \times 100 \tag{2}$$

where q is the biosorption capacity (mg/g), C_0 and C_e are the initial and equilibrium Cr(VI) concentration (mg/L), V is the volume of Cr(VI) solution(L), and m is the weight of the CUS in g.

2.5. Biosorption isotherm models

Biosorption isotherms give the relationship between the adsorbate concentration and the amount of adsorbate biosorbed by the unit mass of biosorbent at a constant temperature under equilibrium condition [32]. The two parameter isotherm models [33] such as Langmuir, Freundlich, Elovich, Temkin, and Jovanovic were used to analyze the equilibrium data obtained in the present study.

2.5.1. Langmuir isotherm

Langmuir isotherm model is based on the assumption that all the biosorption sites have equal adsorbate affinity and that the biosorption at one site does not affect the biosorption at an adjacent site [34]. This isotherm model is used to obtain a maximum biosorption capacity produced from the complete monolayer coverage of biosorbent surface. The Langmuir model can be expressed by the below equation:

$$q_e = \frac{Q_0 K_L C_e}{1 + K_L C_e} \tag{3}$$

where C_e is the equilibrium concentration of the Cr (VI) ion (mg/L), q_e denotes the biosorption capacity at equilibrium (mg/g), Q_0 represents the maximum monolayer biosorption capacity (mg/g), and K_L is the Langmuir isotherm constant (L/mg).

The Langmuir isotherm model expressed in terms of the dimensionless equilibrium constant R_L, referred to as the separation factor or equilibrium parameter as expressed by the following equation:

$$R_L = \frac{1}{1 + K_L C_0} \tag{4}$$

where C_0 represent the initial Cr(VI) concentration (mg/L) and K_L is obtained from the Langmuir plot. The condition based on R_L values are suggested as $0 < R_L < 1$ for favorable, $R_L > 1$ for unfavorable, $R_L = 1$ for linear, and $R_L = 0$ for irreversible biosorption, respectively.

2.5.2. Freundlich isotherm

The Freundlich isotherm model [35] is an empirical model based on biosorption on a heterogeneous surface. The equation is commonly represented by:

$$q_e = K_F C_e^{1/n_F} \tag{5}$$

where K_F and $1/n_F$ are the Freundlich constants, these are characteristics of the system, indicating the adsorption capacity and the adsorption intensity, respectively.

2.5.3. Elovich isotherm

The Elovich model is based on the assumption that the biosorption sites increase exponentially with biosorption process, which entail a multilayer biosorption [36]. The equation of this model is given as follows:

$$\frac{q_e}{q_m} = K_E C_e \exp\left(-\frac{q_e}{q_m}\right) \tag{6}$$

where K_E represent the Elovich equilibrium constant (L/mg), q_m is the Elovich maximum biosorption capacity (mg/g).

2.5.4. Temkin isotherm

This model contains a factor that takes into account of the adsorbent–adsorbate interactions. The model is based on the assumption that due to the adsorbate–adsorbate repulsions, the heat of biosorption of all the molecules in the layer decreases linearly with the coverage of molecules and the biosorption of adsorbate is uniformly distributed [37]. The model is given by the equation:

$$q_e = \frac{RT}{b_T} \ln(A_T C_e) \tag{7}$$

where A_T is the Temkin isotherm equilibrium binding constant (L/mg), b_T denotes Temkin isotherm constant (J/mol).

2.5.5. Jovanovic isotherm

The Jovanovic isotherm [38] assumption is similar to that of the assumption considered in Langmuir isotherm model. It is represented by another approximation for monolayer localized adsorption without lateral interactions:

$$q_e = q_{mj}\left(1 - e^{\left(K_j C_e\right)}\right) \tag{8}$$

where K_j denotes the Jovanovic isotherm constant (L/g), q_{mj} is the maximum biosorption capacity in Jovanovic model (mg/g).

2.6. Biosorption kinetics

The biosorption kinetics analysis is essential for designing over the batch biosorption systems. Kinetic models like pseudo-first-order, pseudo-second-order, and intra-particle diffusion models, respectively, were used to fit the equilibrium data.

2.6.1. Pseudo-first-order

The biosorption rate constant based on the biosorption capacity was determined from the pseudo-first-order kinetic model given by Lagergren [39] and is represented as follows:

$$\log(q_e - q) = \log q_e - \frac{k_1}{2.303} t \tag{9}$$

where q_e and q are the amounts of Cr(VI) biosorbed (mg/g) at equilibrium time and at any time t. k_1 (1/min) is the pseudo-first-order rate constant.

2.6.2. Pseudo-second-order

A pseudo-second-order kinetic model [40] based on the assumption that chemisorption is rate limiting

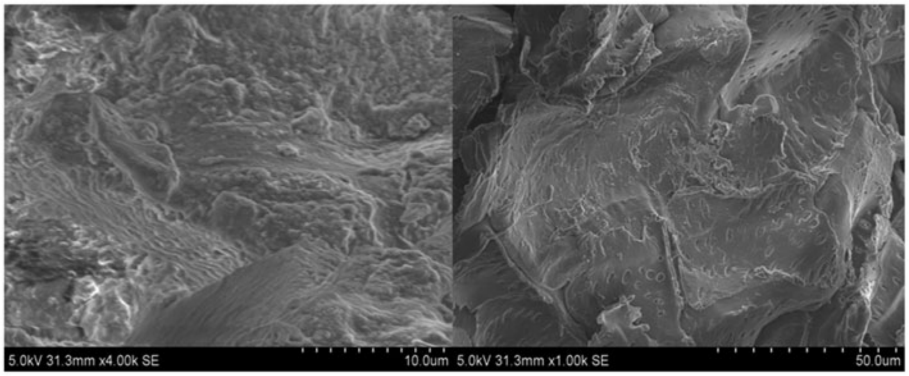

Fig. 1. SEM images of CUS.

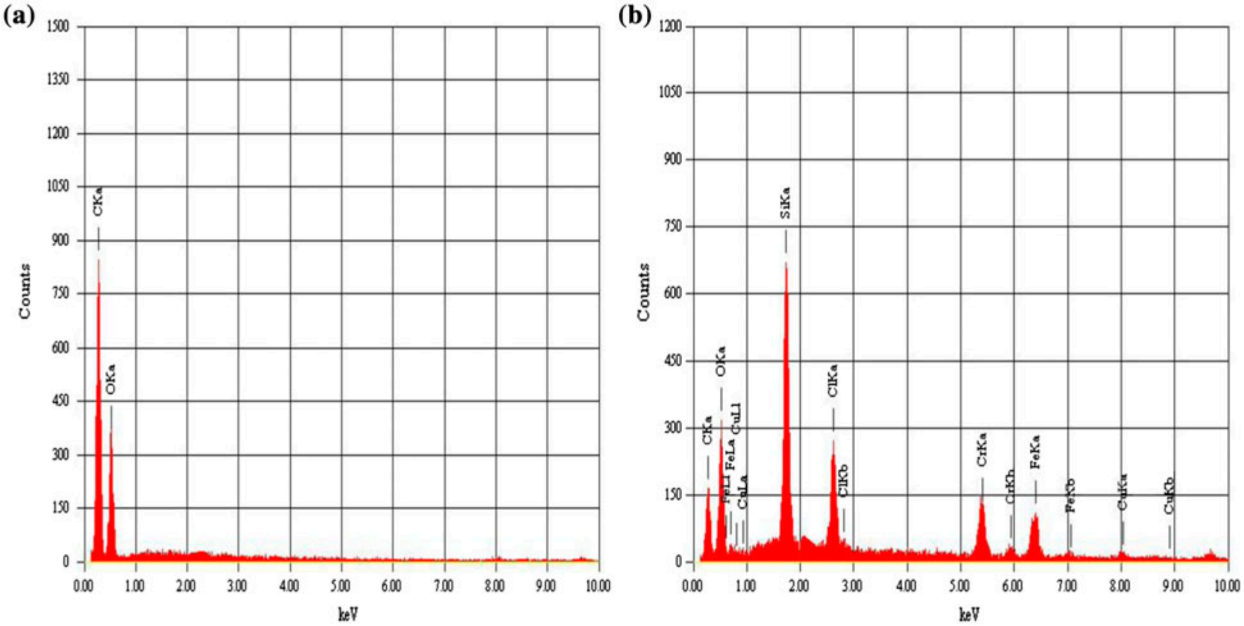

Fig. 2. EDS elemental and spectra mapping of (a) CUS and (b) Cr(VI)-loaded CUS.

step, which involves the valence force sharing or electron exchange between biosorbent and adsorbate. The pseudo-first-order kinetic model is given by the following equation:

$$\frac{t}{q} = \frac{1}{k_2 q_e^2} + \frac{t}{q_e} \tag{10}$$

where k_2 (g/mg min) represents the pseudo-second-order rate constant.

2.6.3. Intra-particle diffusion

The intra-particle diffusion model [41] describes the insights into the mechanisms and rate-controlling steps affecting the biosorption kinetics. The model is represented as follows:

$$q_t = k_{id} t^{1/2} + I \tag{11}$$

where k_{id} is the intra-particle diffusion rate constant (mg/g min$^{1/2}$), I is the intercept.

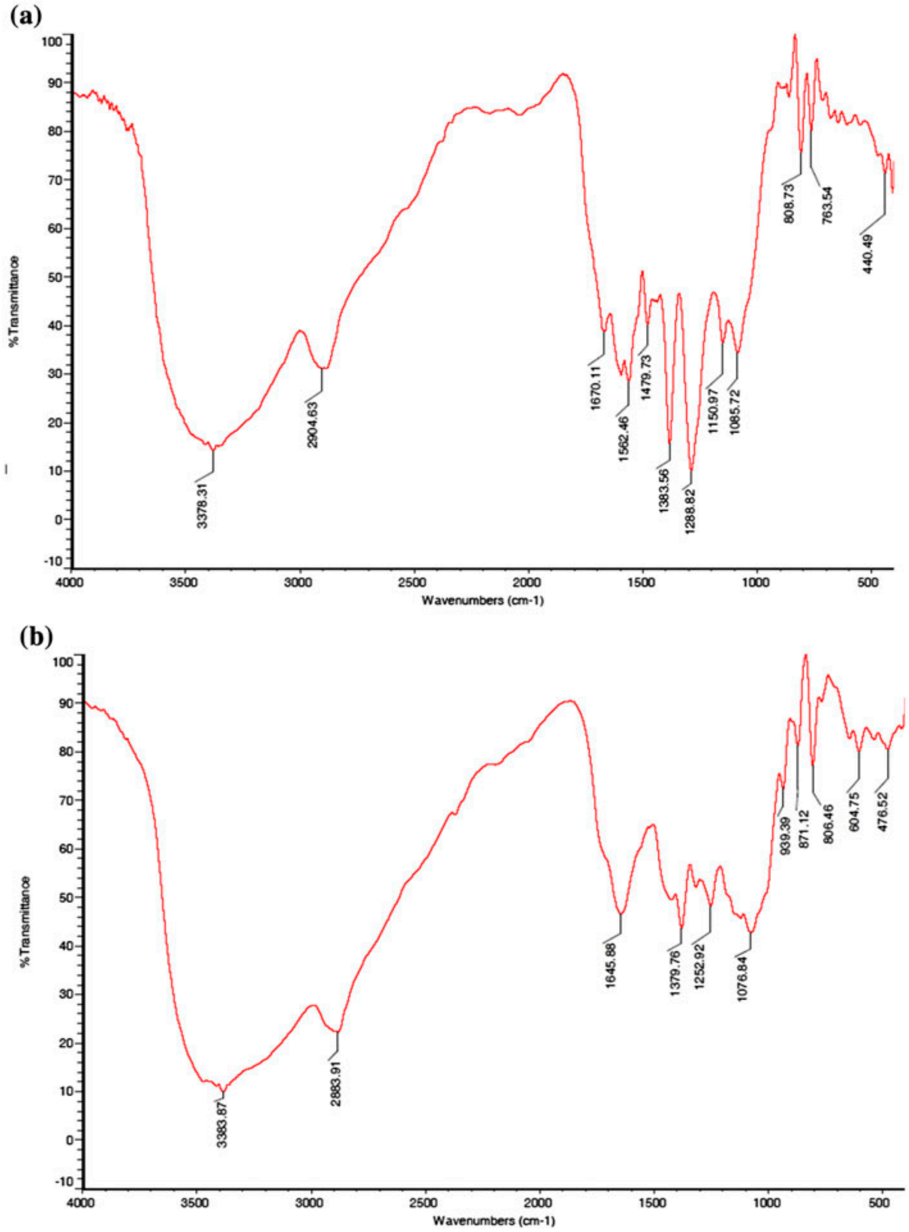

Fig. 3. FT-IR spectra of (a) native and (b) Cr(VI)-loaded CUS.

3. Results and discussion

3.1. Biosorbent characteristics

Scanning electron micrographs (SEM) of the surface structure for CUS are shown in Fig. 1. It is clear from the SEM figures that the CUS surfaces were uneven, rougher, and provided large surface area for hexavalent chromium biosorption. The EDS spectra of native and Cr(VI) loaded CUS are shown in Fig. 2(a) and (b). From these spectra, it was concluded that Cr(VI) has been biosorbed on the surface of the CUS [42].

FT-IR spectra analyses of the native and Cr(VI) loaded CUS (Fig. 3(a) and (b)) were undertaken and results indicated that there are a number of important functional groups on the surface of the CUS. In Fig. 3(a), the absorption peak around 3,378 cm^{-1} indicates the existence of free and intermolecular bonded hydroxyl groups. Moreover, a peak at wave number 2,904 cm^{-1} representing that C–H groups are present on the surface CUS. Other peak at 1,085 cm^{-1} is due to CH_2–OH stretching, and the peak at 1,288 cm^{-1} is related to the C−O stretching in phenols [43,44]. In

Table 1
Effect of CUS particle size on the removal of Cr(VI) at equilibrium

CUS particle size ranges (mm)	Biosorption capacity (mg/g)	% Biosorption
0.180–0.212	12.47	99.80
0.212–0.250	11.74	93.96
0.250–0.300	11.37	90.99

comparison of FT-IR spectra of before Cr(VI) biosorption, FT-IR spectra of Fig. 3(b) represents a clear band shift and intensity decrease at the band regions of C–H, CH_2–OH, and C−O, respectively. These are the functional groups of CUS found to have participated in Cr(VI) biosorption.

3.2. Effect of biosorbent particle size

The effect of CUS particle size on Cr(VI) biosorption capacity and percentage removal is shown in Table 1. The removal of Cr(VI) ions at different particle sizes (0.180–0.212, 0.212–0.250, and 0.250–0.300 mm) indicated that the biosorption capacity and percentage biosorption at the equilibrium increased with the decrease in CUS particle size. The relatively higher biosorption with smaller CUS particle size range may be attributed to the fact that smaller CUS particles have greater surface area. Therefore, CUS particle size range of 0.180–0.212 mm was selected for the experimental purpose.

3.3. Effect of pH

The effect of pH on Cr(VI) biosorption on CUS was studied by varying the pH from 2 to 8. The plot of biosorption capacity (mg/g), % biosorption versus pH is shown in Fig. 4. As seen in Fig. 4, the biosorption capacity and % removal of Cr(VI) decreased with an increase in pH from 2 to 8. This is because, at lower pH the surface of the CUS became positively charged and the electrostatic force of attraction exhibited. But at higher pH, the CUS surface was negatively charged resulted in the repulsion [45]. Therefore, at higher pH values, the surface of CUS becomes deprotonated and results in the decline of Cr(VI) biosorption. For the subsequent study, pH 2 was used as the optimum value.

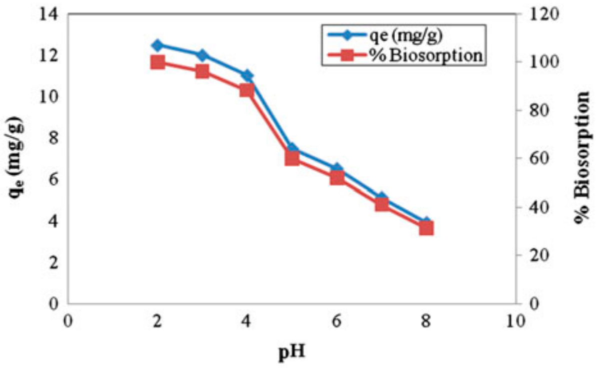

Fig. 4. Effect of pH in biosorption capacity and percentage biosorption of Cr(VI).

3.4. Effect of biosorbent dosage

The effect of the amount of CUS on Cr(VI) biosorption was studied at pH 2 and different amounts of biosorbent dosage in the range 0.05–0.6 g/L (Fig. 5). Biosorption capacity was decreased with an increase in CUS dosage from 0.05 to 0.6 g/L, this is due to the leftover unsaturated biosorption sites. The percentage removal of Cr(VI) removal remained almost same after 0.2 g/L biosorbent dosage. This might be because the biosorption reached equilibrium [46]. Chromium ion biosorption increases with the biosorbent dosage because of an increase in CUS surface area. The biosorption sites available for Cr(VI) removal is directly proportional to CUS surface area.

3.5. Kinetic studies

3.5.1. Effect of initial Cr(VI) concentration and contact time

The amount of Cr(VI) biosorbed on CUS was studied as a function of contact time at different initial Cr(VI) concentrations (50, 100, 150, 200, and 250 mg/L). It is evident from Fig. 6 that the biosorption capacity of CUS toward Cr(VI) removal increased with increase in contact time up to 80 min, then almost attained equilibrium. The removal of Cr(VI) was found to be dependent on the initial Cr(VI) concentration. The amount of Cr(VI) biosorbed by CUS increased with increase in initial Cr(VI) concentration. This is due to higher probability of collision between Cr(VI) ions and CUS resulted in the increased driving force of the concentration gradient [47,48].

The pseudo-first-order, pseudo-second-order, and intra-particle diffusion are the kinetic models used in the present study. The constants of these kinetic models are calculated and represented in Table 2. In comparison of the coefficient of determination of the three kinetic models used, pseudo-second-order kinetic model has the highest value as well the calculated q_e values shows good agreement with the experimental

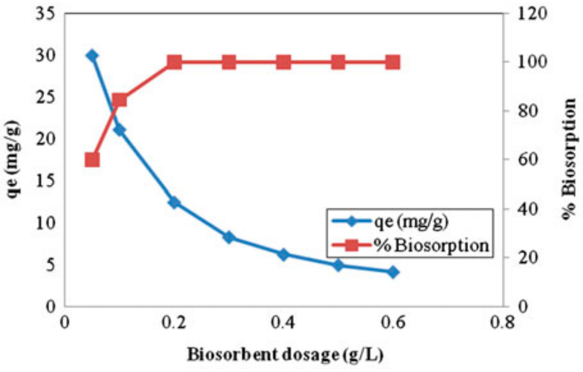

Fig. 5. Effect of biosorbent dosage in biosorption capacity and percentage biosorption of Cr(VI).

data (Table 4). The pseudo-second-order rate constant (k_2) decreases with an increase in initial Cr(VI) concentration due to the increased concentration gradient of the metal ions. Fig. 7 represents the plots of t/q_t against t of the CUS biosorbent at the experimental conditions. Therefore, the kinetic model analysis of CUS toward Cr(VI) revealed that the chemical biosorption is the rate-limiting step.

3.6. Biosorption isotherm

The parameters of biosorption isotherm models were calculated using linear regression analysis and are represented in Table 3. The values of the isotherm

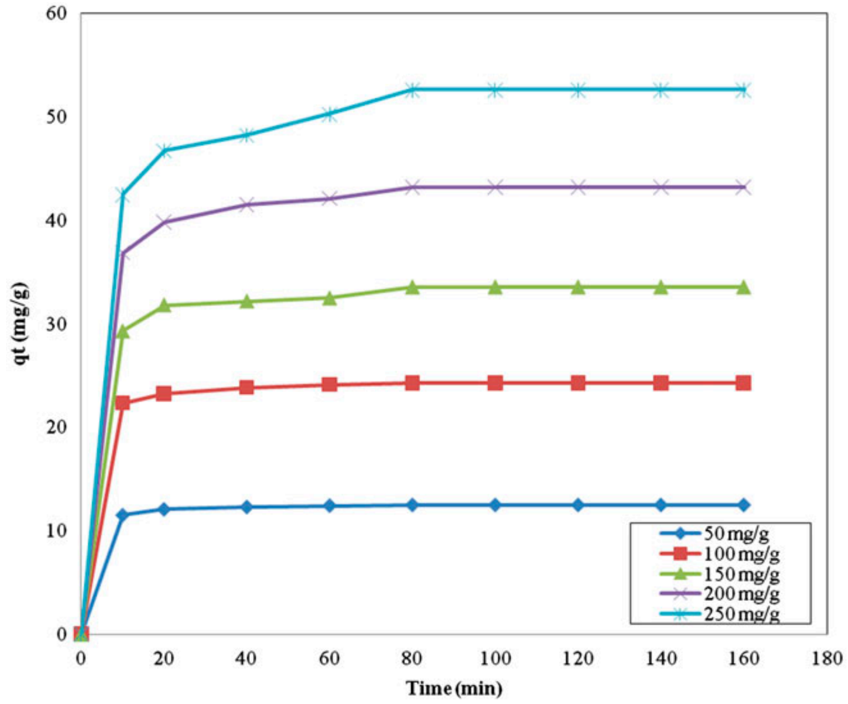

Fig. 6. Effect of contact time on the biosorption of Cr(VI) using CUS for different initial Cr(VI) concentrations.

Table 2
Kinetic constant parameters obtained for Cr(VI) biosorption on CUS

		Pseudo-first-order			Pseudo-second-order			Intra-particle diffusion		
Cr(VI) Conc. (mg/L)	$q_{e(exp)}$ (mg/g)	k_1 (1/min)	$q_{e(cal)}$ (mg/g)	R^2	k_2 (g/mg min)	$q_{e(cal)}$ (mg/g)	R^2	k_{id} (mg/g min$^{1/2}$)	I (mg/g)	R^2
50	12.47	0.0759	4.18	0.849	0.1451	12.65	1.00	0.084	11.57	0.708
100	24.33	0.0690	8.29	0.837	0.0615	25.00	1.00	0.178	22.41	0.763
150	33.60	0.0460	11.29	0.673	0.0233	34.48	0.999	0.382	29.42	0.777
200	43.21	0.0529	17.86	0.806	0.0156	45.45	0.999	0.592	36.82	0.795
250	52.66	0.0141	24.71	0.790	0.0075	55.55	0.999	1.015	41.45	0.854

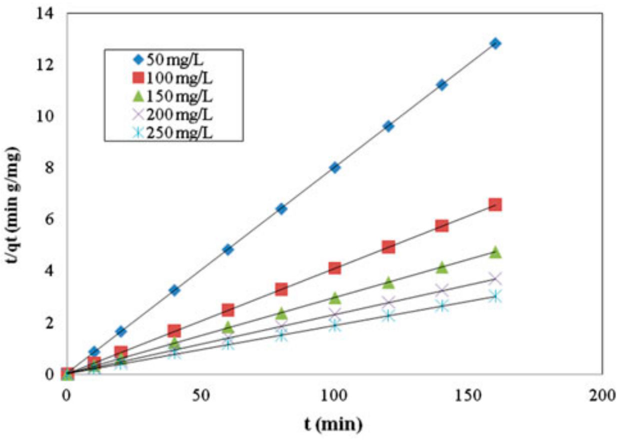

Fig. 7. Plot of the pseudo-second-order model at different initial Cr(VI) concentrations.

Table 4
Comparison of biosorption capacities of various biosorbents for Cr(VI)

Biosorbent	Biosorption capacity (mg/g)	Refs.
Mango sawdust	37.73	[49]
Lathyrus sativus husk	44.5	[50]
Longan seed	35.02	[51]
Powdered Peganum Harmala	10.63	[44]
Tamarind seeds	29.7	[52]
Walnut shell	8.01	[53]
Swietenia mahagoni fruit shell	2.309	[54]
Ficus auriculata leaves	13.33	[55]
Sterculia guttata shell	45.45	[56]
Caryota urens seeds	52.63	Present study
Alligator weed	82.57	[57]
Caryota urens inflorescence	100	[58]
Maize bran	294.13	[59]

model constants and coefficient of determination gives the information of the suitability of the biosorption isotherm models used for the present study. The Langmuir isotherm model better fitted the biosorption equilibrium data. The parameters of this model Q_0 and K_L were found to be as 52.63 mg/g and 0.2753 L/mg. The value of dimensionless equilibrium constant for all the studied Cr(VI) concentrations of 50–250 mg/L was found to be less than one, which pointed out the favorable biosorption of Cr(VI) onto CUS. The values of R_L found for the biosorption study are near to zero which represents the irreversible process. The Freundlich isotherm parameter, the biosorption intensity n_F value of 4.4247 specify that the biosorption of Cr(VI) ions onto CUS is favorable since the value of n_F lies between 1 and 10. The Freundlich isotherm model better described the biosorption equilibrium data. Using Elovich and Jovanovic isotherm model, the maximum biosorption capacity was predicted as 15.62 and 17.58 mg/g (Table 3). The biosorption capacity predicted using Elovich and Jovanovic isotherm model was less compared to the better fitted Langmuir isotherm model. Temkin isotherm

Table 3
Biosorption isotherm constants and coefficient of determination for various biosorption isotherms for Cr(VI) removal using CUS

Biosorption isotherm	Parameters	CUS	Coefficient of determination (R^2)
Langmuir	Q_0 (mg/g)	52.63	
	K_L (L/mg)	0.2753	
	R_L values, C_0 (mg/L)		
	50	0.0677	
	100	0.0350	0.950
	150	0.0236	
	200	0.0178	
	250	0.0143	
Freundlich	K_f (mg/g)/(mg/L)$^{1/n}$	20.27	0.975
	n_F	4.4247	
Elovich	K_E (L/mg)	31.13	0.928
	q_m (mg/g)	15.62	
Temkin	A_T (L/mg)	48.80	0.873
	b_T (kJ/mol)	0.4216	
Jovanovic	q_{mj} (mg/g)	17.58	0.824
	K_j (L/g)	−0.001	

parameter b_T and A_T were calculated and represented in Table 3. The coefficient of determination value of this isotherm indicates that Temkin isotherm model is not fit of equilibrium data as compared with the Langmuir, Freundlich, and Elovich isotherm models, respectively. Based on the coefficient of determination, The Javanovic isotherm model is the least fitted model of among all the biosorption isotherm models used.

4. Conclusions

The present investigation showed that CUS is a potential biosorbent offering greater Cr(VI) treatment than other biosorbents reported in the literature (Table 4). The biosorption of hexavalent chromium by CUS was strongly dependent on biosorbent size, pH, biosorbent dose, contact time, and initial Cr(VI) concentration. The Cr(VI) removal was maximum at pH 2.0. The FT-IR and EDS characterization has shown a distinct difference in the native and Cr(VI) loaded CUS. The biosorption equilibrium data showed better fit to Langmuir and Freundlich isotherm models. The biosorption kinetics was well explained by pseudo-second-order kinetics rather than the pseudo-first-order and intra-particle diffusion kinetic models. Based on the above good results, this waste biomass is recommended as an effective and cheap biosorbent for removal of hexavalent chromium from aqueous solution. But further research has to be focused in the direction of continuous column experiment for the potential application toward the industrials effluents treatment.

Acknowledgments

Authors thank the Research Council for Engineering and Technology Programmes, Kerala State Council for Science, Technology and Environment, India (Grant No. ETP/02/2014/KSCSTE) for their financial support.

List of symbols

A_T — Temkin isotherm equilibrium binding constant (L/mg)
b_T — Temkin isotherm constant (J/mol)
K_L — Langmuir isotherm constant (L/mg)
C_0 — initial Cr(VI) concentration (mg/L)
C_e — Cr(VI) concentration in solution at equilibrium (mg/L)
K_f — Freundlich isotherm constant $(mg/g)/(mg/L)^{1/n}$
K_E — Elovich equilibrium constant (L/mg)
K_j — Jovanovic isotherm constant (L/g)
k_1 — pseudo-first-order rate constant(1/min)
k_2 — pseudo-second-order rate constant (g/mg min)
k_{id} — intra-particle diffusion rate constant $(mg/g\ min^{1/2})$
m — amount of biosorbent (g)
n_F — adsorption intensity
Q_0 — monolayer coverage capacity(mg/g)
q_m — Elovich maximum adsorption capacity (mg/g)
q_{mj} — maximum adsorption capacity in Jovanovic model (mg/g)
q_e — amount of Cr(VI) ions adsorbed per unit mass of biosorbent (mg/g)
R — gas constant (8.314 J/mol K)
R_L — separation factor
V — volume of the solution (L)

References

[1] V.K. Gupta, I. Ali, T.A. Saleh, A. Nayak, S. Agarwal, Chemical treatment technologies for waste-water recycling—An overview, RSC Adv. 2 (2012) 6380–6388.

[2] V.K. Gupta, S.K. Srivastava, D. Mohan, S. Sharma, Design parameters for fixed bed reactors of activated carbon developed from fertilizer waste for the removal of some heavy metal ions, Waste Manage. 17 (1997) 517–522.

[3] A.K. Jain, V.K. Gupta, A. Bhatnagar, Suhas, A comparative study of adsorbents prepared from industrial wastes for removal of dyes, Sep. Sci. Technol. 38 (2003) 463–481.

[4] V.K. Gupta, R. Jain, A. Mittal, T.A. Saleh, A. Nayak, S. Agarwal, S. Sikarwar, Photo-catalytic degradation of toxic dye amaranth on TiO_2/UV in aqueous suspensions, Mater. Sci. Eng. C 32 (2012) 12–17.

[5] A. Mittal, J. Mittal, A. Malviya, D. Kaur, V.K. Gupta, Decoloration treatment of a hazardous triarylmethane dye, Light Green SF (Yellowish) by waste material adsorbents, J. Colloid Interface Sci. 342 (2010) 518–527.

[6] V.K. Gupta, S. Agarwal, T.A. Saleh, Synthesis and characterization of alumina-coated carbon nanotubes and their application for lead removal, J. Hazard. Mater. 185 (2011) 17–23.

[7] V.K. Gupta, R. Jain, A. Nayak, S. Agarwal, M. Shrivastava, Removal of the hazardous dye—Tartrazine by photodegradation on titanium dioxide surface, Mater. Sci. Eng. C 31 (2011) 1062–1067.

[8] A. Mittal, D. Kaur, A. Malviya, J. Mittal, V.K. Gupta, Adsorption studies on the removal of coloring agent phenol red from wastewater using waste materials as adsorbents, J. Colloid Interface Sci. 337 (2009) 345–354.

[9] A. Mittal, J. Mittal, A. Malviya, V.K. Gupta, Adsorptive removal of hazardous anionic dye "Congo red" from wastewater using waste materials and recovery by desorption, J. Colloid Interface Sci. 340 (2009) 16–26.

[10] T.A. Saleh, V.K. Gupta, Column with CNT/magnesium oxide composite for lead(II) removal from water, Environ. Sci. Pollut. Res. 19 (2012) 1224–1228.

[11] A. Mittal, J. Mittal, A. Malviya, V.K. Gupta, Removal and recovery of Chrysoidine Y from aqueous solutions by waste materials, J. Colloid Interface Sci. 344 (2010) 497–507.

[12] V.K. Gupta, A. Nayak, Cadmium removal and recovery from aqueous solutions by novel adsorbents prepared from orange peel and Fe_2O_3 nanoparticles, Chem. Eng. J. 180 (2012) 81–90.

[13] T.A. Saleh, V.K. Gupta, Photo-catalyzed degradation of hazardous dye methyl orange by use of a composite catalyst consisting of multi-walled carbon nanotubes and titanium dioxide, J. Colloid Interface Sci. 371 (2012) 101–106.

[14] H. Khani, M.K. Rofouei, P. Arab, V.K. Gupta, Z. Vafaei, Multi-walled carbon nanotubes-ionic liquid-carbon paste electrode as a super selectivity sensor: Application to potentiometric monitoring of mercury ion(II), J. Hazard. Mater. 183 (2010) 402–409.

[15] S. Karthikeyan, V.K. Gupta, R. Boopathy, A. Titus, G. Sekaran, A new approach for the degradation of high concentration of aromatic amine by heterocatalytic Fenton oxidation: Kinetic and spectroscopic studies, J. Mol. Liq. 173 (2012) 153–163.

[16] N. Sankararamakrishnan, A. Dixit, L. Iyengar, R. Sanghi, Removal of hexavalent chromium using a novel cross linked xanthated chitosan, Bioresour. Technol. 97 (2006) 2377–2382.

[17] B.V. Babu, S. Gupta, Adsorption of Cr(VI) using activated neem leaves: Kinetic studies, Adsorption 14 (2008) 85–92.

[18] G. Gebrehawaria, A. Hussen, V.M. Rao, Removal of hexavalent chromium from aqueous solutions using barks of *Acacia albida* and leaves of *Euclea schimperi* Int. J. Environ. Sci. Technol. 12 (2015) 1569–1580.

[19] EPA Environmental Pollution Control Alternatives EPA/625/5-90/25, EPA/625/4- 89/023, Environmental Protection Agency Cincinaati, OH, USA, 1990.

[20] S. Sugashini, K.M. Meera Sheriffa Begum, Performance of ozone treated rice husk carbon (OTRHC) for continuous adsorption of Cr (VI) ions from synthetic effluent, J. Environ. Chem. Eng. 1 (2013) 79–85.

[21] Z. Djedidi, M. Bouda, M.A. Souissi, R.B. Cheikh, G. Mercier, R.D. Tyagi, J.F. Blais, Metals removal from soil, fly ash and sewage sludge leachates by precipitation and dewatering properties of the generated sludge, J. Hazard. Mater. 172 (2009) 1372–1382.

[22] S.W. Lin, R.M.R. Navarro, An innovative method for removing Hg^{2+} and Pb^{2+} in ppm concentrations from aqueous media, Chemosphere 39 (1999) 1809–1817.

[23] M. Islam, R. Patel, Removal of lead (II) from aqueous environment by a fibrous ion exchanger: Polycinnamamide thorium (IV) phosphate, J. Hazard. Mater. 172 (2009) 707–715.

[24] D.W.O. Connell, C. Birkinshaw, T.F.O. Dwyer, Heavy metal adsorbents prepared from the modification of cellulose: A review, Bioresour. Technol. 99 (2008) 6709–6724.

[25] M.G.A. Korn, J.B. Andrade, D.S. Jesus, V.A. Lemos, M.L.S.F. Bandeira, W.N.L. dos Santos, M.A. Bezerra, F.A.C. Amorim, A.S. Souza, S.L.C. Ferreira, Separation and preconcentration procedures for the determination of lead using spectrometric techniques: A review, Talanta 69 (2006) 16–24.

[26] C.P. Dwivedi, J.N. Sahu, C.R. Mohanty, B. Raj Mohan, B.C. Meikap, Column performance of granular activated carbon packed bed for Pb(II) removal, J. Hazard. Mater. 156 (2008) 596–603.

[27] C.K. Singh, J.N. Sahu, K.K. Mahalik, C.R. Mohanty, B. Raj Mohan, B.C. Meikap, Studies on the removal of Pb (II) from wastewater by activated carbon developed from Tamarind wood activated with sulphuric acid, J. Hazard. Mater. 153 (2008) 221–228.

[28] D.M. Carriazo, D. Arco, C. Martín, V.A. Rives, A comparative study between chloride and calcined carbonate hydrotalcites as adsorbents for Cr(VI), Appl. Clay Sci. 37 (2007) 231–239.

[29] A. Hanif, H.N. Bhatti, M.A. Hanif, Removal and recovery of Cu(II) and Zn(II) using immobilized Mentha arvensis distillation waste biomass, Ecol. Eng. 35 (2009) 1427–1447.

[30] S. Rangabhashiyam, E. Suganya, N. Selvaraju, A.V. Lity, Significance of exploiting non-living biomaterials for the biosorption of wastewater pollutants, World J. Microbiol. Biotechnol. 30 (2014) 1669–1689.

[31] APHA, Standard Methods for the Examination of Water and Waste Water, eighteenth ed., APHA, Washington, DC, 1992.

[32] G. Suresh, B.V. Babu, Removal of toxic metal Cr(VI) from aqueous solutions using sawdust as adsorbent: Equilibrium, kinetics and regeneration studies, Chem. Eng. J. 150 (2009) 352–365.

[33] S. Rangabhashiyam, N. Anu, M.S. Giri Nandagopal, N. Selvaraju, Relevance of isotherm models in biosorption of pollutants by agricultural byproducts, J. Environ. Chem. Eng. 2 (2014) 398–414.

[34] I. Langmuir, The adsorption of gases on plane surfaces of glass, mica and platinum, J. Am. Chem. Soc. 40 (1918) 1361–1367.

[35] H. Freundlich, W. Heller, The Adsorption of cis - and trans -Azobenzene, J. Am. Chem. Soc. 61 (1939) 2228–2230.

[36] S.Y. Elovich, O.G. Larinov, Theory of adsorption from solutions of non electrolytes on solid (I) equation adsorption from solutions and the analysis of its simplest form, (II) verification of the equation of adsorption isotherm from solutions, Assoc Acad Doctrine USSR OTD Khim Lesson 2 (1962) 209–216.

[37] M.J. Tempkin, V. Pyzhev, Kinetics of ammonia synthesis on promoted iron catalysts, A. Physiochim. URSS 12 (1940) 217–222.

[38] D.S. Jovanovic, Physical sorption of gases. I. Isotherms for monolayer and multilayer sorption, Colloid Polym. Sci. 235 (1969) 1203–1214.

[39] S. Lagergren, About the theory of so-called adsorption of soluble substance, Kung Sven Veten Hand 24 (1898) 1–39.

[40] Y.S. Ho, G. McKay, D.A.J. Wase, C.F. Forster, Study of the sorption of divalent metal ions on to peat, Adsorpt. Sci. Technol. 18 (2000) 639–650.

[41] W.J. Weber, J.C. Morris, Advances in water pollution research: Removal of biologically resistant pollutants from waste waters by adsorption, Proceedings of International Conference on Water Pollution Symposium, Pergamon Press, Oxford 2 (1962) 231–266.

[42] S. Rangabhashiyam, N. Selvaraju, Efficacy of unmodified and chemically modified Swietenia mahagoni shell for the removal of hexavalent chromium from simulated wastewater, J. Mol. Liq. 209 (2015) 487–497.

[43] P. Francesca, J. Nohman, T. Franco, E.M. Ma, S. Sebastian, T. Luigi, Biosorption- mediated reduction of Cr(VI) using heterotrophically-grown *Chlorella vulgaris*: Active sites and ionic strength effect, Chem. Eng. J. 231 (2013) 94–102.

[44] K. Rasoul, F. Mehdi, B. Behnam, A.T. Ali, Removal of hexavalent chromium from aqueous solution by granularand powdered Peganum Harmala, Appl. Surf. Sci. 292 (2014) 670–677.

[45] V.K. Gupta, A. Rastogi, Biosorption of hexavalent chromium by raw and acid-treated green alga *Oedogonium hatei* from aqueous solutions, J. Hazard. Mater. 163 (2009) 396–402.

[46] C. Jinfa, Y. Ping, S. Dagang, Y. Sha, Z. Li, H. Lei, L. Bo, Biosorption of Cr(VI) by carbonized *Eupatorium adenophorum* and Buckwheat straw: Thermodynamics and mechanism, Front. Environ. Sci. Eng. 8 (2014) 960–966.

[47] S.S. Baral, S.N. Das, G.R. Chaudhury, P. Rath, Adsorption of Cr (VI) by treated weed *Salvinia cucullata*: Kinetics and mechanism, Adsorption 14 (2008) 111–121.

[48] S. Rangabhashiyam, E. Suganya, N. Selvaraju, Packed bed column investigation on hexavalent chromium adsorption using activated carbon prepared from *Swietenia Mahogani* fruit shells, Desalin. Water Treat. 2015 (2015) 1–8.

[49] V. Vinodhini, N. Das, Relevant approach to assess the performance of sawdust as adsorbent of chromium (VI) ions from aqueous solutions, Int. J. Environ. Sci. Technol. 7 (2010) 85–92.

[50] R. Chakravarty, M.M.R. Khan, A.R. Das, A.K. Guha, Biosorptive removal of chromium by husk of Lathyrus sativus : Evaluation of the binding mechanism, kinetic and equilibrium study, Eng. Life Sci. 13 (2013) 312–322.

[51] Y. Jinbei, Y. Meiqiong, C. Wentao, Adsorption of hexavalent chromium from aqueous solution by activated carbon prepared from longan seed: Kinetics, equilibrium and thermodynamics, J. Ind. Eng. Chem. 21 (2015) 414–422.

[52] G. Suresh, B.V. Babu, Utilization of waste product (tamarind seeds) for the removal of Cr(VI) from aqueous solutions: Equilibrium, kinetics, and regeneration studies, J. Environ. Manage. 90 (2009) 3013–3022.

[53] P. Erol, A. Turkan, Biosorption of chromium(VI) ion from aqueous solutions using walnut, hazelnut and almond shell, J. Hazard. Mater. 155 (2008) 378–384.

[54] S. Rangabhashiyam, N. Anu, N. Selvaraju, Equilibrium and kinetic modeling of chromium (VI) removal from aqueous solution by a novel biosorbent, Res. J. Chem. Environ. 18 (2014) 30–36.

[55] S. Rangabhashiyam, E. Nakkeeran, N. Anu, N. Selvaraju, Biosorption potential of a novel powder, prepared from *Ficus auriculata* leaves, for sequestration of hexavalent chromium from aqueous solutions, Res. Chem. Intermed. 1 (2015) 8405–8424.

[56] S. Rangabhashiyam, N. Selvaraju, Adsorptive remediation of hexavalent chromium from synthetic wastewater by a natural and $ZnCl_2$ activated *Sterculia guttata* shell, J. Mol. Liq. 207 (2015) 39–49.

[57] X. SongWang, Y. Ping Tang, S. Rong Tao, Kinetics, equilibrium and thermodynamic study on removal of Cr (VI) from aqueous solutions using low-cost adsorbent Alligator weed, Chem. Eng. J. 148 (2009) 217–225.

[58] S. Rangabhashiyam, N. Selvaraju, Evaluation of the biosorption potential of a novel *Caryota urens* inflorescence waste biomass for the removal of hexavalent chromium from aqueous solutions, J. Taiwan Inst. Chem. Eng. 47 (2015) 59–70.

[59] S.H. Hasan, K.K. Singh, O. Prakash, M. Talat, Y.S. Ho, Removal of Cr(VI) from aqueous solutions using agricultural waste ‘maize bran’, J. Hazard. Mater. 152 (2008) 356–365.